Suplemento de la Revista Mexicana de Física **3** 0308037 (2022) 1–4

Double triangle cusps relevant to $P_c(4312)^+$, $P_c(4380)^+$, and $P_c(4457)^+$

S. X. Nakamura

University of Science and Technology of China,
Hefei 230026, People's Republic of China.
State Key Laboratory of Particle Detection and Electronics (IHEP-USTC),
Hefei 230036, People's Republic of China.
e-mail: satoshi@ustc.edu.cn

Received 12 March 2021; accepted 19 January 2022

A novel scenario is proposed for hidden charm pentaquark (P_c)-like structures in $\Lambda_b^0 \to J/\psi p K^-$. The scenario is based on kinematical singularities arising from double triangle mechanisms. Anomalous threshold cusps due to the singularities are, compared with ordinary $\sum_c^{(*)} \bar{D}^{(*)}$ one-loop thresh-old cusp, significantly more singular. It is demonstrated that an interference among the double triangle mechanisms and other common mechanisms generates peaks very similar to the $P_c(4312)^+$, $P_c(4380)^+$, and $P_c(4457)^+$ peak structures. While hadron molecules and compact pentaquarks have been common models to explain the P_c states, the present model is a completely different one. The present model includes only one pentaquark state $P_c(4440)^+$. However, we find that the $P_c(4440)^+$ width and strength are significantly smaller than those from the LHCb analysis. The P_c^+ signals are searched for in J/ψ photoproduction but not found. A search was also made in $\Lambda_b^0 \to J/\psi p \pi^-$ data, finding only a possible $Pc(4440)^+$-like signal. The present model is consistent with the experimental situation.

Keywords: Pentaquark; kinematical singularities.

DOI: https://doi.org/10.31349/SuplRevMexFis.3.0308037

1. Introduction

Recently, three pentaquark-like structures have been observed in the LHCb experiment for $\Lambda_b^0 \to J/\psi p K^-$ [1]. The pentaquarks are named as $P_c(4312)^+$, $P_c(4440)^+$, and $P_c(4457)^+$. The masses of the pentaquarks are located close to and below the $\Sigma_c(2455)\bar{D}^{(*)}$ thresholds[i]. This fact seems consistent with a picture that P_c^+'s are $\Sigma_c(2455)\bar{D}^{(*)}$ molecules (bound states), although a compact pentaquark picture is not fully excluded. P_c^+'s as resonances or bound states should appear in various processes. On the other hand, P_c^+'s might also be interpreted as a kinematical effect and, in this case, P_c^+'s would not appear in other processes where the kinematical condition is different from $\Lambda_b^0 \to J/\psi p K^-$. One test case is the photoproduction of J/ψ from a nucleon target. The GlueX Collaboration measured this process, finding a null result [2, 3]. This result may favor the kinematical effect interpretation, while one could still argue that the P_c^+'s weakly couple with photons.

Recently, we identified double triangle (DT) diagrams (Fig. 1a)) that can occur kinematically at the classical level [4]. According to the Coleman-Norton theorem, the DT diagrams can hit the leading kinematical singularities [5], causing anomalous threshold cusps. As we will show, compared with the ordinary $\Sigma_c(2455)\bar{D}^{(*)}$ one-loop threshold cusp, these anomalous cusps are significantly more singular. Thus the anomalous cusps might appear as resonance-like structures. We here demonstrate that the $P_c(4312)^+$, $P_c(4380)^+$, and $P_c(4457)^+$ peak structures are well fitted by a combination of the DT, one-loop, and direct decay amplitudes. We will see that the interference among these mechanisms plays a crucial role. Only the $P_c(4440)^+$ peak in the LHCb data requires a resonant mechanism. The $P_c(4440)^+$ width and strength from our fit are much smaller than those from the LHCb analysis. We will also discuss that this newly proposed P_c interpretation is consistent with the experimental situation for other processes where P_c signals are expected.

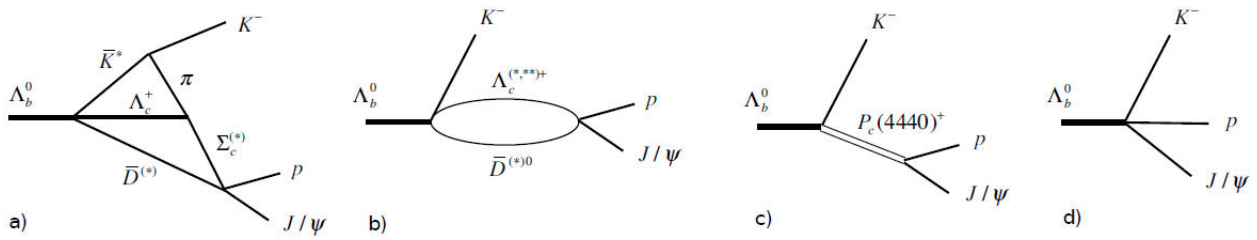

FIGURE 1. $\Lambda_b^0 \to J/\psi p K^-$ mechanisms considered in this work: a) double triangle; b) one-loop; c) $P_c(4440)^+$; d) direct decay. Figures taken from Ref. [4]. Copyright (2021) APS.

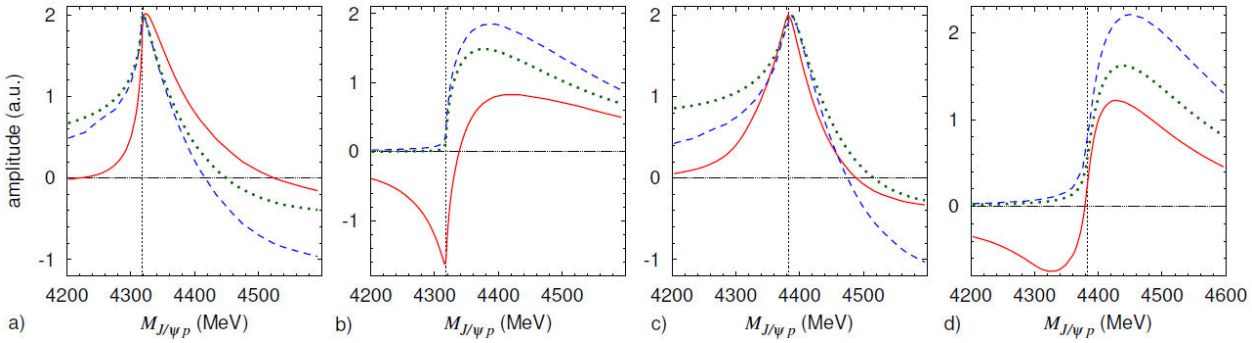

FIGURE 2. Amplitudes of double triangle mechanisms. a) [(b)] The real [imaginary] part of the mechanism of Fig. 1a) with $\Sigma_c^{(*)}\bar{D}^{(*)} = \Sigma_c^+\bar{D}^0$ is shown by the red solid curve. They reduce to the blue dashed ones if we use $m_{\Lambda_c^+} = 3$ GeV. The green dotted curves are from the $\Sigma_c^+\bar{D}^0$ one-loop amplitude. A normalization has been made so that the real parts of all the amplitudes have the same maximum value. The $\Sigma_c^+\bar{D}^0$ threshold is indicated by the dotted vertical lines. Σ_c^+ in these amplitudes is replaced by Σ_c^{*+}, giving the amplitudes shown in the panels c) and d). Figures taken from Ref. [4]. Copyright (2021) APS.

2. Model

The diagrams shown in Fig. 1 are considered for describing $\Lambda_b^0 \to J/\psi p K^-$. For the weak decays of $\Lambda_b^0 \to \Lambda_c^{(*,**)+}\bar{D}^{(*)}\bar{K}^{(*)}$ in Figs. 1a), b), we assume the dominance of color-favored quark-level processes. The Breit-Wigner form is used to describe the $P_c(4440)^+$ mechanism of Fig. 1c). A direct decay of Fig. 1d) is considered for each partial wave. With a notation of J^P being the spin-parity of $J/\psi p$, the $J^P = 1/2^-, 3/2^-, 1/2^+$, and $3/2^+$ partial waves are taken into account (see Ref. [4] for a complete set of formulas of the relevant amplitudes). We expect that the Y_c and $\bar{D}^{(*)}$ strongly interact in the one-loop and DT processes. This effect is taken into account by using a single-channel scattering model with a contact interaction. Other coupled-channel effects are assumed to be hidden in complex couplings that are fitted to the data.

3. Results

3.1. Singular double triangle amplitudes

We show in Figs. 2a), b) the DT amplitude by the red solid curves. This DT mechanism includes $\Sigma_c^+\bar{D}^0\,(1/2^-)$. Around the $\Sigma_c^+\bar{D}^0$ threshold, the leading singularity of the DT amplitude causes a singular behavior. We also show an ordinary $\Sigma_c^+\bar{D}^0$ one-loop threshold cusp by the green dotted curves. The DT amplitude is clearly more singular. If we use a hypothetically heavy value (3 GeV) for the Λ_c^+ mass, the DT amplitude should behave as the ordinary $\Sigma_c^+\bar{D}^0$ threshold cusp. The blue dashed curves confirm this expectation. We also make a similar plot by replacing Σ_c^+ in the DT amplitude with Σ_c^{*+}, as given in Figs. 2c), d). The obtained DT amplitude including $\Sigma_c^{*+}\bar{D}^0$ is a bit away from the leading singularity. Therefore, its behavior is less singular, compared with the leading one shown in Figs. 2a), b). Yet, it is still more singular, compared with the ordinary one-loop threshold cusp.

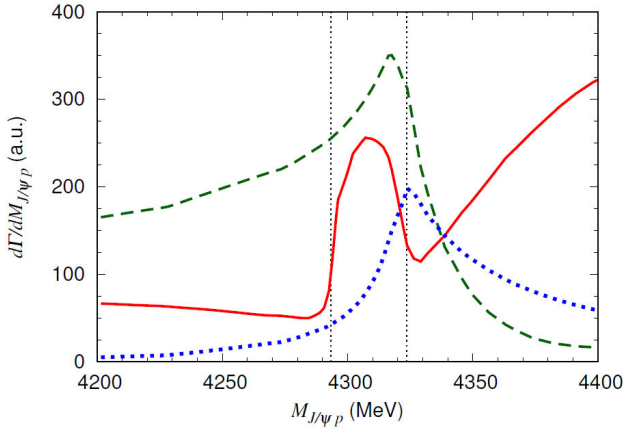

FIGURE 3. The $P_c(4312)^+$ peak, in the differential decay width ($d\Gamma/dM_{J/\psi p}$), formed from interfering various amplitudes. The double triangle amplitude with the $\Sigma_c\bar{D}$ pair alone generates the blue dotted curve. The green dashed curve includes a direct decay amplitude in addition. The further inclusion of the $\Lambda_c^+\bar{D}^{*0}$ one-loop mechanism results in the red solid curve. The $\Lambda_c^+\bar{D}^{*0}$ and $\Sigma_c(2455)^{++}D^-$ thresholds are indicated by the dotted vertical lines.

How does a DT amplitude create a P_c peak? From the DT amplitude that includes $\Sigma_c\bar{D}$ alone, we get the blue dotted curve in Fig. 3. As expected from Fig. 2, the blue dotted curve peaks at the $\Sigma_c\bar{D}$ threshold. However, the $P_c(4312)$ peak is below the threshold. Then we include a direct decay mechanism and obtain the green dashed curve. Now the peak is slightly below the threshold. We further include the $\Lambda_c^+\bar{D}^{*0}$ one-loop mechanism, and obtain the red solid curve. Now a good agreement with the $P_c(4312)$ peak is reached.

3.2. Analyzing the LHCb data

Our model for $\Lambda_b^0 \to J/\psi p K^-$ includes: (i) DT amplitudes with $\Sigma_c(2455)\bar{D}\,(1/2^-)$, $\Sigma_c(2520)\bar{D}\,(3/2^-)$, $\Sigma_c(2455)\bar{D}^*\,(1/2^-)$, $\Sigma_c(2455)\bar{D}^*\,(3/2^-)$, $\Sigma_c(2520)\bar{D}^*\,(1/2^-)$, and $\Sigma_c(2520)\bar{D}^*\,(3/2^-)$; (ii) one-loop amplitudes

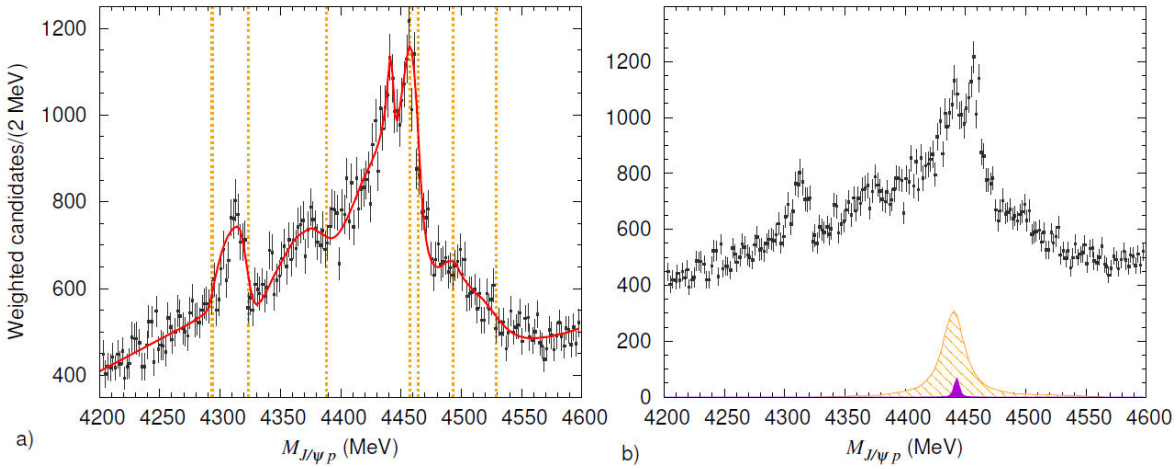

FIGURE 4. The $J/\psi p$ invariant mass ($M_{J/\psi p}$) distribution for $\Lambda_b^0 \to J/\psi p K^-$. a) Our full model is shown by the red solid curve. The dotted vertical lines indicate various thresholds. From the left, they are $\Lambda_c^+\bar{D}^{*0}$, $\Sigma_c(2455)^{++}D^-$, $\Sigma_c(2520)^{++}D^-$, $\Lambda_c(2595)^+\bar{D}^0$, $\Sigma_c(2455)^{++}D^{*-}$, $\Lambda_c(2625)^+\bar{D}^0$, and $\Sigma_c(2520)^{++}D^{*-}$ thresholds. The data are from Ref. [1]; $\cos\theta_{P_c}$-weighted samples. b) The contribution from the $P_c(4440)^+$ mechanism. The LHCb analysis found the $P_c(4440)^+$ contribution as given by the orange striped peak. Our model's $P_c(4440)^+(3/2^-)$ contribution is given by the solid violet peak; no interference included. Figure is (partly) taken from Ref. [4]. Copyright (2021) APS.

with $\Lambda_c^+\bar{D}^{*0}\,(1/2^-)$, $\Lambda_c(2595)^+\bar{D}^0\,(1/2^+)$, and $\Lambda_c(2625)^+\bar{D}^0\,(3/2^+)$; (iii) $P_c(4440)^+$ resonant amplitude; (iv) direct decay amplitudes. The full model possesses 26 fitting parameters in total, as below. Each mechanism in the items (i)-(iii) has an adjustable complex overall factor: 2×10 parameters. Each of the direct decays in the item (iv) has a real coupling: 4 parameters. The $P_c(4440)^+$ mass and width give two fitting parameters. We also have one parameter from a repulsive strength of the $\Lambda_c^+\bar{D}^{*0}$ interaction. Since the absolute normalization of the full amplitude is arbitrary, the number of the free parameters is reduced by 1.

Regarding the $Y_c\bar{D}^{(*)}(J^P)$ interactions, we first examine each if an attraction or repulsion is preferred by the fit. Attractions are favored for $\Sigma_c(2455)\bar{D}\,(1/2^-)$, $\Sigma_c(2520)\bar{D}\,(3/2^-)$, $\Sigma_c(2455)\bar{D}^*\,(1/2^-)$, $\Sigma_c(2455)\bar{D}^*\,(3/2^-)$, $\Lambda_c(2595)^+\bar{D}^0\,(1/2^+)$, $\Lambda_c(2625)^+\bar{D}^0\,(3/2^+)$, while repulsions are for $\Sigma_c(2520)\bar{D}^*\,(1/2^-)$, $\Sigma_c(2520)\bar{D}^*\,(3/2^-)$, $\Lambda_c^+\bar{D}^{*0}\,(1/2^-)$. For the attractive interactions, we use couplings so that they have $a\sim0.5$ fm (a: scattering length). Regarding the repulsive interactions, the $\Lambda_c^+\bar{D}^{*0}\,(1/2^-)$ coupling is fitted to the data. We obtained the coupling strength such that $a\sim-0.4$, -0.2, and -0.05 fm for $\Lambda\sim0.8$, 1, and $1.5-2$ GeV, respectively (Λ: common cutoff value used in form factors). Then, the other repulsive $Y_c\bar{D}^{(*)}(J^P)$ channels use the same coupling strength. Since the spectrum peak positions are determined by the kinematical effects, they do not sensitively depend on the a values. We use the common cutoff value of $\Lambda=1$ GeV in the form factors included in every interaction vertex. Changing the cutoff value does not significantly change our result. Only the direct decay amplitudes include different cutoff values so that they have a phase-space-like $M_{J/\psi p}$ distribution.

Our calculation is compared with the LHCb data [1] as shown in Fig. 4a); the calculated results have been smeared with the experimental resolution. Our full model (red solid curve) fits the data well. The kinematical effects caused by the mechanisms considered create the peak structures of the $P_c(4312)^+$, $P_c(4380)^+$, and $P_c(4457)^+$. In our model, a resonance pole is only from $P_c(4440)^+$; in the figure, $J^P=3/2^-$ is chosen for $P_c(4440)^+$. We examined the cutoff dependence by varying it in the range of $\Lambda=0.8-2$ GeV. We also examined other J^P for $P_c(4440)^+$ such as $J^P=1/2^\pm$ and $3/2^\pm$. In either of the cases, we do not find a significant change of the fit quality.

We show in Fig. 4b), the $P_c(4440)^+(3/2^-)$ contribution. The violet solid peak is from our analysis; no interference effect included. Our fit gives the Breit-Wigner mass of 4443.1 ± 1.4 MeV and width of 2.7 ± 2.4 MeV. On the other hand, the LHCb analysis [1] obtained the mass of $4440.3\pm1.3^{+4.1}_{-4.7}$ MeV and width of $20.6\pm4.9^{+8.7}_{-10.1}$ MeV. The width values are rather different between LHCb analyses and ours. The $P_c(4440)^+$ contribution from the LHCb analysis is ~22 larger than ours as seen by comparing the orange striped peak (LHCb) and the violet solid peak (ours) in Fig. 4b). Different fitting strategies end up with this large difference. In the LHCb analysis, $P_c(4440)^+$ and $P_c(4457)^+$ contributions are incoherently summed to fit the large structure at $M_{J/\psi p}\sim4450$ MeV. In our case, a large part of the structure is described by the kinematical effects, and only the remaining small spike is fitted by the $P_c(4440)^+$ and its interference.

Another evidence for P_c^+ was also found by the LHCb in $\Lambda_b^0\to J/\psi p\pi^-$. In Fig. 3(b) of Ref. [6], an enhancement is seen in the $M_{J/\psi p}$ bin of $P_c(4440)^+$. For the other P_c^+'s, however, no enhancement is discernible. Actually, our model

gives a picture consistent with this observation because: (i) a relevant DT mechanism does not exist in $\Lambda_b^0 \to J/\psi p\pi^-$; (ii) the $P_c(4440)^+$ excitation mechanism can be shared by $\Lambda_b^0 \to J/\psi p\pi^-$. This $\Lambda_b^0 \to J/\psi p\pi^-$ data may challenge some other P_c^+ models. Yet, the limited quality of the P_c^+ signals in $\Lambda_b^0 \to J/\psi p\pi^-$ does not allow any conclusive statement. The LHCb Run II data on $\Lambda_b^0 \to J/\psi p\pi^-$, expected to come soon, would be interesting.

Recent LHCb data provided another interesting information on P_c. They studied $B_s^0 \to J/\psi p\bar{p}$ and found another pentaquark-like peak, called $P_c(4337)$, while finding no evidence for $P_c(4312)$ [7]. This new data is also consistent with our model discussed in this paper. This point is detailed in Ref. [8]. In this reference, we pointed out that $P_c(4312)^+$ and $P_c(4337)^+$ can be created by different interference patterns between the $\Lambda_c\bar{D}^*$ and $\Sigma_c\bar{D}$ (anomalous) threshold cusps.

4. Summary

In this work, a model is developed for $\Lambda_b^0 \to J/\psi pK^-$, and the LHCb's $M_{J/\psi p}$ distribution data is analyzed. The double triangle and other common mechanisms interfere with each other to develop structures that fit well the P_c^+ structures. In our analysis, only $P_c(4440)^+$ is treated as a resonance. Compared with the result from the LHCb analysis, the $P_c(4440)^+$ width and strength are much smaller. While hadron molecules and compact pentaquarks models have been often used to interpret the P_c^+ peaks, our interpretation proposed here is a completely different one. We here showed for the first time that the double triangle mechanisms can cause resonance-like structures. This is a general finding, and we expect double triangle mechanisms to create also other resonance-like structures. Indeed, one of such cases has been found and discussed recently [9].

Acknowledgments

This work is in part supported by National Natural Science Foundation of China (NSFC) under contracts U2032103 and 11625523, and also by National Key Research and Development Program of China under Contracts 2020YFA0406400.

---

i. The hadron naming scheme of Ref. [2] will be used. However, we often use abbreviations such as Σ_c, Σ_c^*, Λ_c^*, and Λ_c^{**} for $\Sigma_c(2455)^{+(++)}$, $\Sigma_c(2520)^{+(++)}$, $\Lambda_c(2595)^+$, and $\Lambda_c(2625)^+$, respectively; Y_c refers to $\Lambda_c^{(*,**)}$ and $\Sigma_c^{(*)}$ collectively. The notation $BM(J^P)$ stands for a baryon (B) and a meson (M) paired in a spin-parity J^P.

1. R. Aaij *et al.*, Observation of a Narrow Pentaquark State, $Pc(4312)^+$, and of the Two-Peak Structure of the $Pc(4450)^+$, *Phys. Rev. Lett.* **122** (2019) 222001.

2. P.A. Zyla *et al.* (Particle Data Group), The Review of Particle Physics, *Prog. Theor. Exp. Phys.* **2020** (2020) 083C01.

3. A. Ali *et al.* (GlueX Collaboration), First measurement of near-threshold J/ψ exclusive photoproduction off the proton, *Phys. Rev. Lett.* **123** (2019) 072001.

4. S.X. Nakamura, $Pc(4312)^+$, $Pc(4380)^+$, and $Pc(4457)^+$ as double triangle cusps, *Phys. Rev. D* **103** (2021) L111503.

5. R. J. Eden, P. V. Landshoff, D. I. Olive and J. C. Polkinghorne, *The Analytic S-Matrix*, Cambridge University Press, Cambridge, England, 1966.

6. R. Aaij *et al.*, Evidence for exotic hadron contributions to $\Lambda_b^0 \to J/\psi p\pi^-$ decays, *Phys. Rev. Lett.* **117** (2016) 082003.

7. R. Aaij *et al.*, Evidence for a new structure in the $J/\psi p$ and $J/\psi\bar{p}$ systems in $B_s^0 \to J/\psi\phi p\bar{p}$ decays, arXiv:2108.04720.

8. S.X. Nakamura, A. Hosaka, and Y. Yamaguchi, Pc(4312)+ and Pc(4337)+ as interfering $\sum_c \bar{D}$ and $\Lambda_c\bar{D}^*$ threshold cusps, *Phys. Rev. D* **104** (2021) L091503.

9. S.X. Nakamura, X structures in $B^+ \to J/\psi\phi K^+$ as ordinary and anomalous threshold cusps, arXiv:2111.05115,